Resources Processing 59 : 33–41 (2012)

RESOURCES PROCESSING

Original Paper

Characterization of Calcium-doped Silica Gel Prepared in an Aqueous Solution

Dang Viet QUANG[1,3], Jin-Koo PARK[2], Jong-Kil KIM[2], Gideon ELINEEMA[1], Godlisten N. SHAO[1], Jae Eun LEE[1] and Hee Taik KIM[1]*

[1]Department of Fine Chemical Engineering, Hanyang University, 1271 Sa3-dong, Sangnok-gu, Ansan-si, Gyeonggi-do 426-791, Republic of Korea
[2]E&B Nanotech. Co., Ltd., Republic of Korea
[3]Institute of Environmental Technology, Vietnam Academy of Science and Technology, 18 Hoang Quoc Viet, Cau Giay, Hanoi, Vietnam

Abstract

In this study, calcium-doped silica was prepared by modifying sodium silicate-based silica gel in an aqueous solution of $Ca(OH)_2$. Silica gels with less than 1 mm in size with different pH values were treated in $Ca(OH)_2$ solution at concentrations ranging from 2 to 20 g/L and aged at 25, 60, and 90°C for 40 min. The BET surface area of the silica gel decreased while its pore size increased considerably after modification in $Ca(OH)_2$ solution. The pH of 5% calcium-doped silica in water ranged from about 8.5 to 10, depending on the pH of silica gel, the aging temperature, and the concentration of the $Ca(OH)_2$. When the concentration of the $Ca(OH)_2$ solution was 20%, needle-like crystals of calcium silicate hydrate formed over the surface of silica gel.

Key words: Silica gel, Calcium silicate hydrate, Calcium-doped silica, Anticorrosion

1. Introduction

Silica gel is a porous material with high surface area, high pore volume, and large pore diameter. This material not only possesses durable and biocompatible properties, but also contains a large number of silanol groups (≡Si-OH) on its surface[1]. Through these silanol groups, the surface of silica gel can be easily modified with either organic functional groups or inorganic cations[2–4]. Calcium ions have been widely used to synthesize both calcium-doped silica and calcium silicate composites[5–9].

Calcium-doped silica (CS) was synthesized and its functionality as a catalyst, drug carrier, and anticorrosion pigment was investigated[5,10–12]. In normal phase liquid chromatography, silica gel modified with calcium showed a considerable increase in its retention and selectivity[8]. Samart et al. (2010) reported the use of calcium-supported mesoporous silica as an effective catalyst for transesterification of soybean oil with a conversion yield of 95% at a reaction temperature of 60°C for 8 h[10]. Since calcium silicate composite is a bioactive, biocompatible, and degradable material, it has emerged as a potential candidate for drug carrier and biomedical applications[13–15].

Products ranging from consumer items and equipment to construction materials are usually exposed to corrosive environments during use. Consequently, corrosion reduces both the functionality and the appearance of products; in serious cases, catastrophic failure may occur, with the potential for financial loss and even personal injury. Thus, protecting products from corrosion is extremely important. In order to protect products from environmental degradation, anticorrosive coating layers consisting of organic polymers and inorganic pigments are usually applied on their surface, particularly on the surface of steel substrates[16]. Chromate compounds are effective conventional pigments, which enhance the passivation of steel surfaces and can work over a wide

Paper presented at the 9th Japan/Korea International Symposium on Materials Science and Resources Recycling, 30 May–1 June 2011, Osaka, Japan
Accepted 20 February, 2012
*e-mail: khtaik@hanyang.ac.kr

pH range. However, chromate pigments are toxic materials that should be replaced by eco-friendly pigments with the same protective ability[17–19]. Various pigments such as CS and mixtures thereof, zinc phosphate, and iron oxide proved to be good choices due to their high anticorrosive and non-toxic properties[20–23]. In a previous publication, the authors reported CS has a better anticorrosive performance than red iron oxide that closely approaches the durability of chromate pigments[12].

CS is usually prepared by modifying silica substrates with Ca^{2+} ions in aqueous solution[3,8,24]. Ca^{2+} ions can be attached to silica matrices by a reaction with silanol groups on the surface[3,4]. Although the interaction between silica gel and $Ca(OH)_2$ has been studied, the effects of $Ca(OH)_2$ concentration and reaction temperature on the porous structure of the resultant CS have not been well investigated. In this work, we prepared CS from sodium silicate-based silica gel and $Ca(OH)_2$ in an aqueous solution and investigated the pH and porous structure of the resulting products.

2. Materials and Methods

2.1 Synthesis of calcium-doped silica gel

Silica gel was synthesized via a sol-gel method as described in our previous publication[25] using sodium silicate $Na_2O{\cdot}3.4SiO_2$ (24%, Shinwoo Materials Co., Ltd.) as a silica precursor. Sodium silicate solution was mixed with a 40% H_2SO_4 (Duksan Pure Chemicals Co., Ltd.) solution through a nozzle at 25°C (room temperature, RT) in order to generate silica hydrogel in excessively acidic conditions. This hydrogel was aged at RT for three days and then washed with tap water to remove excessive H_2SO_4 and to control the pH of the silica gel. Three kinds of silica gel with a pH of 4, 6, or 7 were selected and denoted Gel4, Gel6, and Gel7, respectively.

The washed silica gels were smashed to sizes below 1 mm for modification with $Ca(OH)_2$ (Chameleon Reagent). An aqueous solution of $Ca(OH)_2$ (200 ml) at concentrations of 2, 5, 10, or 20% was placed in an 1 L beaker and 20 g of silica gel was added. This $Ca(OH)_2$/silica suspension was aged for 40 min at 25, 60, or 90°C. The resulting $Ca(OH)_2$/silica suspension was filtered and dried at 130°C for 5 h and then ground to produce CS powder. The CS samples synthesized from the selected silica gel at different temperatures and concentrations of $Ca(OH)_2$, are presented in Tables 1 and 2.

2.2 Characterizations

The CS powder was homogenously dispersed in deionized water to yield a slurry concentration of 5%, then the pH was measured using a pH/ISE meter (pH-250L). TEM images were taken using field electron scanning transmission electron microscopy (FE-STEM; JEOL 2000 FX model). The chemical composition of the CS was determined using an energy-dispersive X-ray (EDX) component attached to the FE-STEM instrument. The Brunauer-Emmett-Teller (BET) surface area and the porosity of the samples were studied using a nitrogen adsorption instrument (Micromeritics Tristar II). The samples were degassed at 250°C for 3 h before analysis. X-ray diffraction (XRD) was performed with an XRD-6000 (Shimazu) operating at 40 kV, 100 mA with Cu/Kα radiation ($\gamma = 1.54059$ Å). Thermal gravimetric and differential thermal analysis (TG-DTA) was conducted using a TG/DTA6100 (Seiko Exstar 6000) at a

Table 1 Variations in surface area and porosity with aging temperature

Sample name	$Ca(OH)_2$ concentration (g/L)	Aging temperature (°C)	BET surface area (m^2/g)	Pore volume (cm^3/g)	Pore size (nm)
Gel 4	0	25	736	0.31	2.9
CS4-01	5	25	397	0.86	7.9
CS4-02	5	60	357	0.79	8.4
CS4-03	5	90	341	0.95	12.0
Gel 6	0	25	674	0.52	3.5
CS6-02	5	25	381	0.76	7.0
CS6-09	5	60	349	0.84	8.8
CS6-06	5	90	328	0.9	10.3
Gel 7	0	25	650	0.53	3.5
CS7-01	5	25	352	0.8	8.6
CS7-02	5	60	340	0.8	8.7
CS7-03	5	90	302	0.9	11.9

Table 2 Variations in surface area and porosity of Gel 6 with $Ca(OH)_2$ concentration

Sample name	$Ca(OH)_2$ contents (%)		Aging temperature (°C)	BET surface area (m^2/g)	Pore volume (cm^3/g)	Pore size (nm)
	Nominal	*In Ca/SiO₂*				
CS6-01	2	1.86	25	438	0.78	6.3
CS6-02	5	3.71	25	381	0.76	7.0
CS6-03	10	5.91	25	284	0.84	11.7
CS6-04	20	10.39	25	275	0.83	11.8
CS6-05	2	1.90	90	367	0.92	9.2
CS6-06	5	3.22	90	328	0.9	10.3
CS6-07	10	5.6	90	268	0.88	13.0
CS6-08	20	10.38	90	234	0.82	14.1

heating rate of 10°C/min in air at temperatures ranging from 25 to 1000°C.

3. Results

3.1 pH values of CS

The reactions used to synthesize CS are described in equations (1) and (2)[4,24]. According to those reactions, the pH values of CS mostly depend on excessive $Ca(OH)_2$ concentration and unsaturated ≡Si-Ca-OH bonds. CS may become calcium silicate, which is near neutral pH due to its low solubility if the $Ca(OH)_2$ molecules form full bonds with silica matrices in the reaction (2). When the free $Ca(OH)_2$ concentration is low, the pH will be dominated by unsaturated ≡Si-Ca-OH species as indicated in (3).

$$\equiv\text{Si-OH} + \text{Ca(OH)}_2 \leftrightarrow \equiv\text{Si-O-Ca-OH} + \text{H}_2\text{O} \quad (1)$$

$$\equiv\text{Si-O-Ca-OH} + \equiv\text{Si-OH} \leftrightarrow \equiv\text{Si-O-Ca-O-Si}\equiv + \text{H}_2\text{O} \quad (2)$$

$$\equiv\text{Si-O-Ca-OH} \leftrightarrow \equiv\text{Si-O-Ca}^+ + \text{OH}^- \quad (3)$$

In this study, the pH of the 5% CS solutions varied as a function of the $Ca(OH)_2$ concentrations (Fig. 1a). As the $Ca(OH)_2$ concentrations increased from 2 g/L to 20 g/L, the pH increased from 8.5 to 10 at both aging temperatures, 25°C and 90°C. The pH of CS synthesized from 2 g/L $Ca(OH)_2$ and aged at 25°C were almost the same as that aged at 90°C and the trend was similar for CS synthesized from 20 g/L $Ca(OH)_2$ and aged at 25°C and 90°C. However, when the $Ca(OH)_2$ concentrations were between 2–20 g/L, the pH of CS aged at 25°C were always higher than that aged at 90°C. The results are presented in Fig. 1a.

No evidence of excessive $Ca(OH)_2$ in samples was observed on XRD analyses even though the concentrations were increased up to 20 g/L and

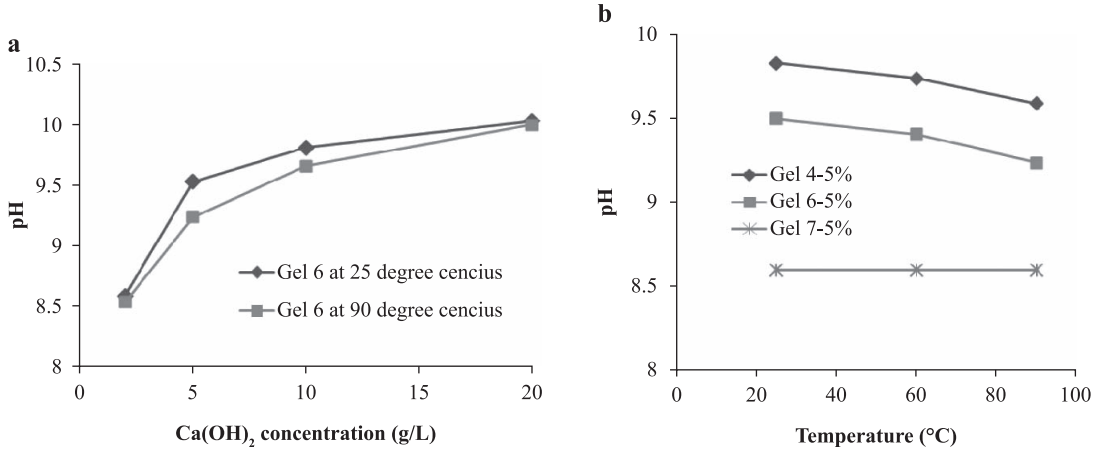


Fig. 1 Variation in the pH of 5% CS slurry with $Ca(OH)_2$ concentration (a) and aging temperature (b).

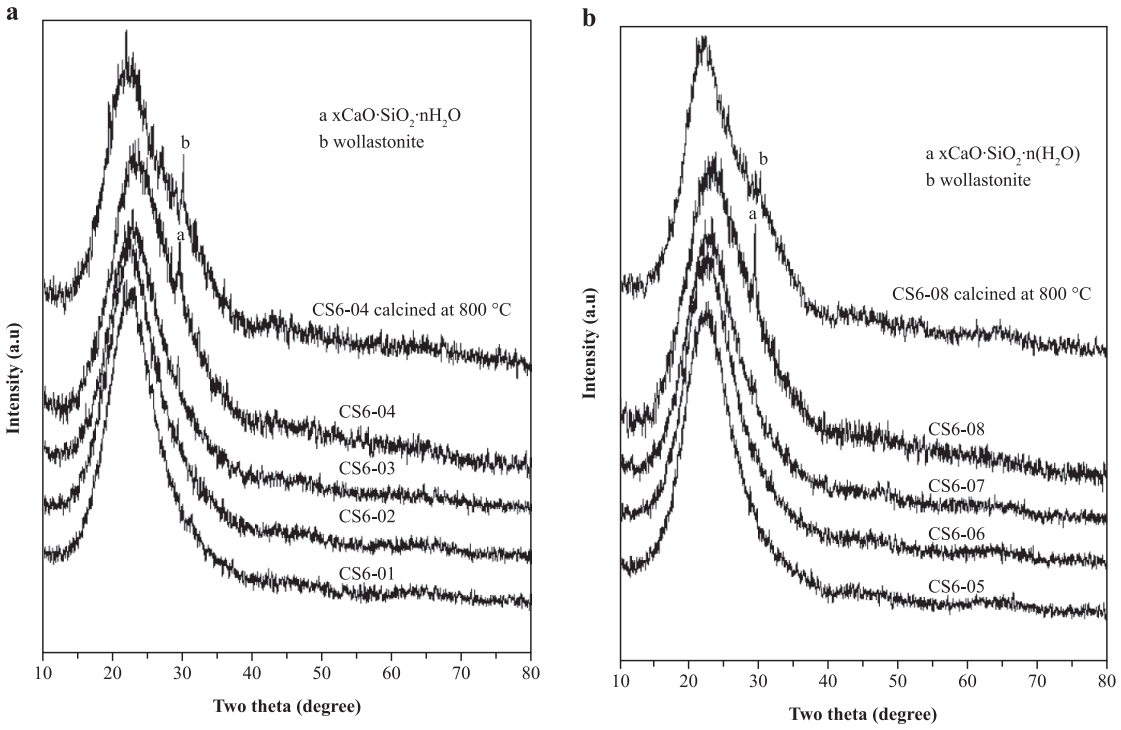


Fig. 2 XRD patterns of CS synthesized from gel 6 with different $Ca(OH)_2$ concentration at 25°C (a) and 90°C (b).

samples were aged at both 25 and 90°C (Fig. 2). Since the concentration of free $Ca(OH)_2$ was negligible, the pH of CS was mostly attributed to ≡Si-Ca-OH groups, which were located on the surface and in the pores of silica and ready to release OH^- and Ca^{2+} ions[26]. Therefore, the variations in pH, in fact, were related to the formation of ≡Si-O-Ca-O-Si≡ and ≡Si-O-Ca-OH species in the CS structure. When the $Ca(OH)_2$ concentration was 2 g/L, the modification process was completed with reaction (2) irrespective of the aging temperature because the molar ratio of $Ca(OH)_2$/≡Si-OH was small. The concentration of the ≡Si-O-Ca-OH species quickly came to equilibrium at both 25 and 90°C, which is why the pH values were the same for the samples aged at those temperatures.

When the $Ca(OH)_2$ concentrations were between 2–20 g/L, the modification followed both reactions (1) and (2). However, the condensation rate increased at an elevated temperature[24], which led to a quick decrease in the concentration of ≡Si-O-Ca-OH species in the samples aged at 90°C. This is why the pH values of the samples aged at 90°C were lower than those of the samples aged at 25°C. At a $Ca(OH)_2$ concentration of 20 g/L, the reaction (1) was likely to reach the equilibrium point within the aging time (40 min) with a high concentration of ≡Si-O-Ca-OH species since there was a high ratio of $Ca(OH)_2$/≡Si-OH. In addition, the concentration of free Ca^{2+} ions in solution increased along with the rise in $Ca(OH)_2$[26] and was not negligible at 20 g/L of $Ca(OH)_2$. Therefore, the pH values recorded were about 10 for both samples aged at 25 and 90°C.

In order to examine the effects of both the aging temperature and the pH of silica gel on the pH of 5% CS solutions, the concentration of $Ca(OH)_2$ was kept constant at 5 g/L while the CS was aged at 25, 60, and 90°C for 40 min. Variations in the pH of the 5% CS slurry as the aging temperature and the pH of silica gel changed are shown in Fig. 1b. It is obvious that the pH of the slurry increased as the pH of the silica gel decreased. The variations in the pH values with the aging temperature were the same as discussed above for gels 4 and 6; these variations were reduced as the temperature increased. However, when the pH of the silica gel was 7 the pH values of CS did not depend on the aging temperature.

The activity of ≡Si-OH groups varies with the pH of silica gel[1]. Accordingly, the activity of ≡Si-OH decreases at lower pH. At low pH, equation (4) moves to the left side, which reduces the

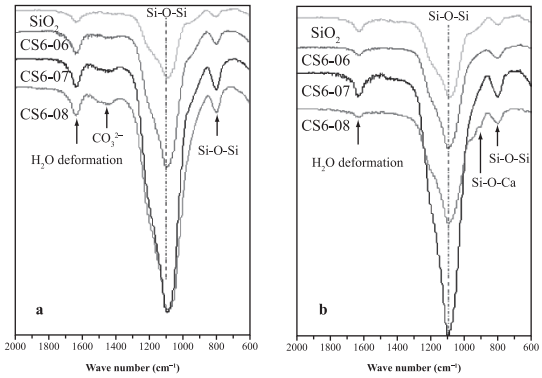


Fig. 3 FT-IR spectra of synthesized from gel 6 with different $Ca(OH)_2$ concentration dried at 180°C (a) and calcined at 800°C (b).

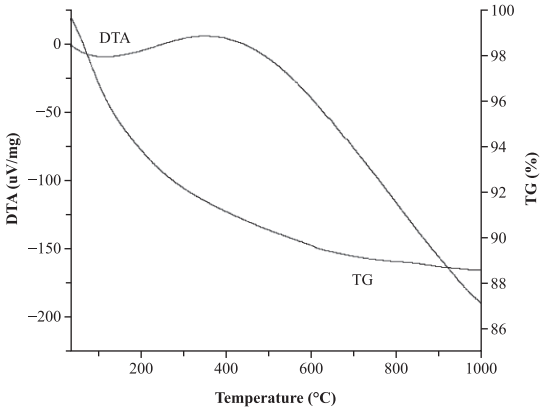


Fig. 4 DTA and TG diagram of CS aging at 25°C (CS6-04)

activity of the ≡Si-OH groups. Therefore, the condensation described in equation (2) decreases and the pH of CS increases due to the higher concentration of the ≡Si-O-Ca-OH species. It was previously reported that the equilibrium of the reaction between ≡Si-OH and $Ca(OH)_2$ can be attained in a short time even at low temperature[4]. Moreover, larger pore volume and more defined pore size in Gel7 were favorable for the transportation and reaction of $Ca(OH)_2$. Thus, the equilibrium of the modification reaction of Gel7 was likely established within 40 min of aging at temperatures from 25 to 90°C. This explains why the pH values of CS synthesized from Gel7 remained constant, while the aging temperatures were elevated.

$$\equiv\text{Si-OH} \leftrightarrow \equiv\text{Si-O}^- + \text{H}^+ \quad (4)$$

3.2 Formation of calcium silicate hydrates

Calcium ions can react with soluble silica formed under basic conditions and with silanol groups located on the silica gel surface to produce various calcium silicate species depending on the molar ratio of Ca^{2+} ions to silica[6,24]. Different species may yield different performance in applications due to their properties. For anticorrosive applications, CS synthesis aims to form the ≡Si-O-Ca-OH species, which is capable of releasing Ca^{2+} from the silica substrate[25,27,28]. The ≡Si-O-Ca-O-Si≡ species, which has low solubility, high durability, and biocompatible and degradable properties, is suitable for use as a bioactive carrier[29].

X-ray diffraction studies provided good evidence of the formation of calcium silicate hydrate ($xCaO{\cdot}SiO_2{\cdot}nH_2O$). Fig. 2 shows XRD patterns of CS synthesized from Gel6 with different $Ca(OH)_2$ concentrations at 25 and 90°C. It is apparent in this figure that the intensity of the diffraction peak at 29.7° increased with increasing $Ca(OH)_2$ concentration at both 25 and 90°C, suggesting the existence of the calcium silicate hydrate phase in the samples. Since this peak is similar to that corresponding to the diffraction of $CaCO_3$, additional confirmation was obtained by acquiring XRD diffraction patterns of CS6-04 and CS6-08 calcined at 800°C for 3 h. The calcinations of those samples resulted in the shift of the peak to 30°C. This result indicates the presence of $CaO{\cdot}SiO_2{\cdot}nH_2O$, which was transformed to wollastonite at 800°C[30].

The formation of Si-O-Ca bonds was investigated by FT-IR spectroscopy. Fig. 3 shows FT-IR spectra of CS6-06, CS6-07, and CS6-08 dried at 180°C and calcined at 800°C, respectively. The bands at 1630, 1100 and 800 cm^{-1} found in all samples belong to characteristic vibrations of silica substrate. The bands located at 1630 cm^{-1} is assigned to vibration of bonding H_2O molecules. The bands found at 1100 and 800 cm^{-1} correspond to Si-O-Si stretching and Si-O-Si bending vibration, respectively. The CS samples dried at 180°C have a broad band at 1450 cm^{-1} attributing to the vibration of CO^{2-}_3 groups and its intensity increases with the increase of $Ca(OH)_2$ concentration (Fig. 3a). This result indicates that $CaCO_3$ have been formed during the modification. As samples were calcined at 800°C, the band at about 1450 cm^{-1} disappeared due to the decomposition of $CaCO_3$. However, a new bands at about 900 cm^{-1} is observed in the sample treated with 20% $Ca(OH)_2$ (Fig. 3b). This band is corresponding to Si-O-Ca bonds in wollastonite[6,7]. This result suggests that the Si-O-Ca bonds have been formed by the modification of silica gel with the $Ca(OH)_2$ solution.

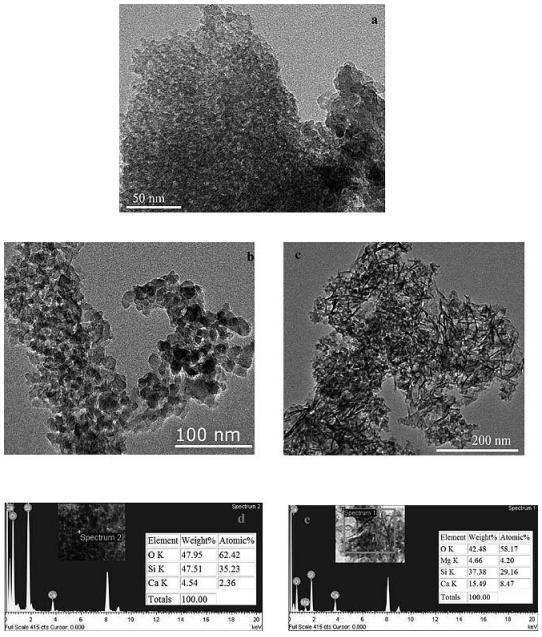


Fig. 5 TEM images of Gel 6 (a), its CS synthesized at 25°C with $Ca(OH)_2$ concentrations of 5 g/L (b) and 20 g/L (c), and EDS spectra of the selected areas of those CS samples: 5 g/L (d) and 20 g/L (e).

DTA-TG measurements were performed on CS6-04 and CS6-08. A representative DTA-TG diagram is shown in Fig. 4 because they are the same for these two samples. In this figure, only one broad endothermic peak was recorded at 350°C, corresponding to the dehydration of the calcium silicate hydrate and absorbed water in silica pores. This result suggests that the concentration of $Ca(OH)_2$ and $CaCO_3$ in the prepared samples is negligible. The presence of calcium silicate hydrate was also clearly observed in the TEM images shown in Fig. 5. The condensed structure of the silica gel was loosened and the sizes of the silica primary particles increased after aging with the 5% $Ca(OH)_2$ solution. In particular, when the $Ca(OH)_2$ concentration was increased to 20 g/L, needle-like crystals over the surface of silica gel were observed. The needle-like crystals are assumed to be calcium silicate hydrate as mentioned in previous reports[31].

EDS spectra of selected areas of CS synthesized from 5 to 20% $Ca(OH)_2$ solutions were also acquired (Figs. 5d and e). Calcium was detected in both samples, with and without needle-like crystals over the surface of the silica gel. This finding suggests that calcium ions were successfully doped in the silica gel via the aqueous method. The calcium silicate hydrate was formed over the surface of the silica gel as the $Ca(OH)_2$ concentration increased to 20%.

3.3 Variations in BET surface area and CS porosity

The BET surface area and porous properties are extremely important in the use of silica and its compounds as fillers or carriers. The BET surface area and porosity of the silica gel and CS samples were investigated in this study using the nitrogen adsorption-desorption method. Isotherms and pore size distributions of the silica gel and CS prepared from Gel4, Gel6, and Gel7 at different temperatures are presented in Fig. 6 while the average values of BET surface area, pore volume, and pore size are reported in Table 1. It is evident from Fig. 6 that the isotherms of silica gel are distinctively different from those of the CS samples. The isotherm loop of Gel4 suggests that silica gel had a low porous structure at pH 4. The pore size distribution of this sample was quite narrow as shown in Fig. 6a (inset). The average pore diameter and pore volume given in Table 1 are 2.9 nm and 0.31 cm^3/g, respectively. The isotherm loops and amounts of absorbed nitrogen for Gel6 and Gel7 were greater than those of Gel4. These results imply that the washing process resulted in an increased pore size and pore volume in the silica gel. The hysteresis loops and pore size distributions were nearly the same for Gel6 and Gel7 due to the similarity of their porous structures. In fact, those silica samples had the same average pore size (Table 1). In addition, their hysteresis loops had desorption branches steeper than the adsorption branches, corresponding to the H2 type of IUPAC classification. This suggests that the silica gel has a condensed structure with narrow and less-defined pore channels[32]. The result is consistent with the TEM observations presented in Fig. 5 a in which Gel6 exhibits a condensed structure with indistinguishable pores. In addition to the increase in porosity, the BET surface area of the silica gel gradually reduces with the washing time increased. This phenomenon is due to the Ostwald ripening effect, which caused the dissolution of small silica particles, while the large particles became larger[33].

In general, the amount of absorbed nitrogen was markedly higher for all CS samples compared to that of the silica gel (Fig. 6). This indicated that the porosity of the silica gel increased after doping with calcium ions, and is consistent with evidence in Fig. 6 (insets) that the pore size distributions in all CS samples broadened and shifted to a predominance of larger pores. Specifically, the average pore volume and pore size increased considerably,

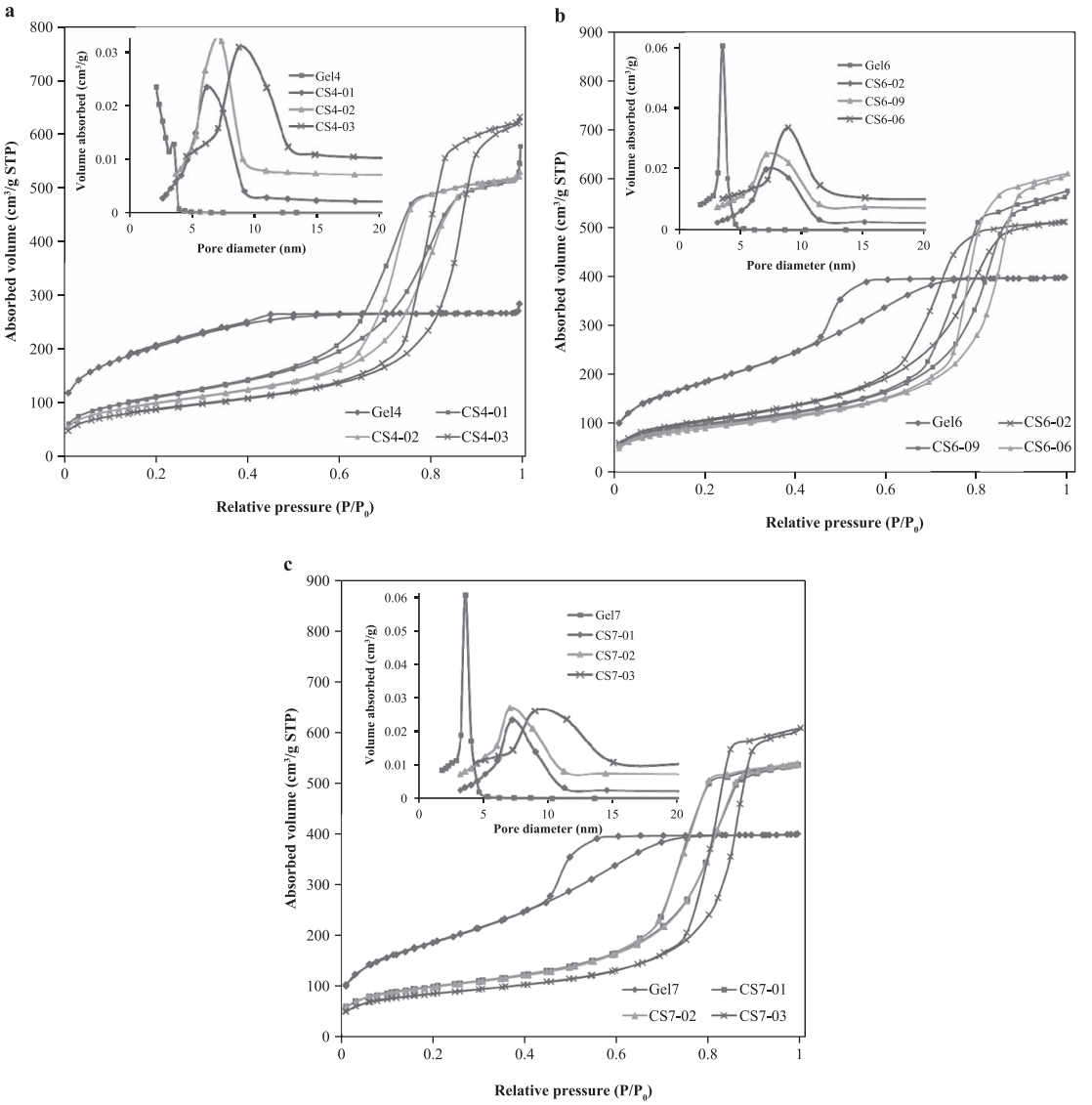


Fig. 6 Nitrogen absorption-desorption isotherms and pore size distribution (inset) of CS synthesized from gel 4 (a), gel 6 (b), and gel 7 (c) at different temperature.

however the BET surface area declined as the aging temperature increased (Table 1). While the reduction in BET surface area is mostly regulated by the Ostwald ripening effect as mentioned above, the increase in pore size is dominated by the curvature characteristic of the pore channels. A convex surface with high chemical potential tends to dissolve whereas a concave surface possessing low chemical potential tends to be enlarged[33]. In addition, changes in the porous structure are also accelerated by aging at high temperature and pH because such aging conditions cause an increase in the solubility of silica gel[34,35].

The effects of $Ca(OH)_2$ concentrations and aging temperatures on the porous structure of CS were also investigated. Table 2 lists the average BET surface area, pore volume, and pore size of CS synthesized from Gel6 with $Ca(OH)_2$ concentrations ranging from 2% to 20% aged at 25 and 90°C. The obtained data indicates that the BET surface area of the CS declined. Conversely, the pore size increased with the rise in $Ca(OH)_2$ concentration. These results prove that the $Ca(OH)_2$ content has considerable influence on the transfor-

mation of the porous structure of the silica gel. The transformation is even more significant at elevated aging temperature. Specifically, in 20% $Ca(OH)_2$ solution, the BET surface area and pore size are 275 m^2/g and 11.8 nm at 25°C; however, at 90°C they are 234 m^2/g and 14.1 nm, respectively (Table 2). As discussed, the solubility of silica gel increased at the higher aging temperature. Moreover, the higher concentration of $Ca(OH)_2$ caused a rise in solution pH, leading to enhancement of silanol group activity. Consequently, the Ostwald ripening effect was enhanced and the transformation of the porous structure of CS intensified.

4. Conclusion

CS was synthesized by modifying sodium silicate-based silica gel with $Ca(OH)_2$ in an aqueous solution. The pH values of 5% CS in water varied from about 8.5 to 10 depending on the $Ca(OH)_2$ concentration and the pH of the silica gel. As the $Ca(OH)_2$ content increased, the calcium silicate hydrate crystals formed over the surface of silica gel. The aging temperature and the concentration of $Ca(OH)_2$ markedly enhanced the transformation of the porous structure of CS; the pore size of silica gel increased from about 3 to 12 nm after aging 40 min in 5% $Ca(OH)_2$ solution at 90°C, and the pore size increased up to 14.1 nm when the silica gel was treated in 20% $Ca(OH)_2$ solution at 90°C.

In conclusion, this study has proposed a facile route to synthesize CS in an aqueous solution that may be suitable for large-scale production. The prepared CS can be used as anticorrosive filler in paint or as a bioactive carrier.

Acknowledgement

This work was supported by a grant from Energy Technology Innovation (ETI) R&D Program, the Ministry of Knowledge Economy, S. Korea.

References

1. R.K. Iler: The chemistry of silica, in, Wiley, New York (1979)
2. D.V. Quang, P.B. Sarawade, A. Hilonga, J.-K. Kim, Y.G. Chai, S.H. Kim, J.-Y. Ryu, H.T. Kim: Preparation of amino functionalized silica micro beads by dry method for supporting silver nanoparticles with antibacterial properties, Colloids and Surfaces A, Physicochemical and Engineering Aspects, **389**, pp. 118–126 (2011)
3. L. Armelao, A. Bassan, R. Bertoncello, G. Biscontin, S. Daolio, A. Glisenti: Silica glass interaction with calcium hydroxide: a surface chemistry approach, Journal of Cultural Heritage, **1**, pp. 375–384 (2000)
4. S.A. Greenberg: The Chemisorption of Calcium Hydroxide by Silica, The Journal of Physical Chemistry, **60**, pp. 325–330 (1956)
5. X. Li, L. Zhang, X. Dong, J. Liang, J. Shi: Preparation of mesoporous calcium doped silica spheres with narrow size dispersion and their drug loading and degradation behavior, Microporous and Mesoporous Materials, **102**, pp. 151–158 (2007)
6. A. Meiszterics, L.s. Rosta, H. Peterlik, J.n. Rohonczy, S. Kubuki, P.t. Henits, K. Sinkoì: Structural Characterization of Gel-Derived Calcium Silicate Systems, The Journal of Physical Chemistry A, **114**, pp. 10403–10411 (2010)
7. A. Meiszterics, K. Sinkó: Sol–gel derived calcium silicate ceramics, Colloids and Surfaces A: Physicochemical and Engineering Aspects, **319**, pp. 143–148 (2008)
8. M. Okamoto, K. Nobuhara, D. Ishii: Effect of calcium-modified silica on retention and selectivity in normal-phase liquid chromatography, Journal of Chromatography A, **697**, pp. 153–158 (1995)
9. I.A. Simonova, A. Freni, G. Restuccia, Y.I. Aristov: Water sorption on composite "silica modified by calcium nitrate", Microporous and Mesoporous Materials, **122**, pp. 223–228 (2009)
10. C. Samart, C. Chaiya, P: Reubroycharoen, Biodiesel production by methanolysis of soybean oil using calcium supported on mesoporous silica catalyst, Energy Conversion and Management, **51**, pp. 1428–1431 (2010)
11. A. Kalendová, D. Veselý, J. Stejskal, M. Trchová: Anticorrosion properties of inorganic pigments surface-modified with a polyaniline phosphate layer, Progress in Organic Coatings, **63**, pp. 209–221 (2008)
12. L.W. Vasconcelos, I.C.P. Margarit, O.R. Mattos, F.L. Fragata, A.S.B. Sombra: Inhibitory properties of calcium exchanged silica epoxy paintings, Corrosion Science, **43**, pp. 2291–2303 (2001)
13. S. Ni, J. Chang, L. Chou: A novel bioactive porous CaSiO3 scaffold for bone tissue engineering, Journal of Biomedical Materials Research Part A, **76A**, pp. 196–205 (2006)
14. W. Xia, J. Chang: Well-ordered mesoporous bioactive glasses (MBG): A promising bioactive drug delivery system, Journal of Controlled Release, **110**, pp. 522–530 (2006)
15. N. Zhang, J.A. Molenda, J.H. Fournelle, W.L. Murphy, N. Sahai: Effects of pseudowollastonite (CaSiO3) bioceramic on in vitro activity of human mesenchymal stem cells, Biomaterials, **31**, pp. 7653–7665 (2010)
16. V.I. Pokhmurs'kyi, I.M. Zin, L.M. Bilyi, S.B. Lyon: Specific Features of the Anticorrosive Action of a Mixture of Nontoxic Pigments in an Epoxy Coating on Steel, Materials Science, **37**, pp. 123–127 (2001)

17. M. Bethencourt: Inhibitor properties of “green” pigments for paints, Progress in Organic Coatings, **46**, pp. 280–287 (2003)
18. D. Veselý, A. Kalendova: Anticorrosion efficiency of ZnxMgyAl2O4 core–shell spinels in organic coatings, Progress in Organic Coatings, **62**, pp. 5–20 (2008)
19. D. Veselý, A. Kalendova, P. Kalenda: A study of diatomite and calcined kaoline properties in anticorrosion protective coatings, Progress in Organic Coatings, **68**, pp. 173–179 (2010)
20. I.M. Zin’, L.M. Bilyi, I.P. Gnyp, M.B. Ratushna: Protective Action of Phosphate and Calcium-Containing Pigments under the Conditions of the Stress Corrosion Fracture of Steels, Materials Science, **40**, pp. 605–610 (2004)
21. I. Zin: Corrosion inhibition of galvanized steel with inorganic pigments, Materials Science, **35**, pp. 874–878 (1999)
22. V.I. Pokhmurs’kyi, I.M. Zin’, S.B. Lyon: Inhibition of corrosion by a mixture of nonchromate pigments in organic coatings on galvanized steel, Materials Science, **40**, pp. 383–390 (2004)
23. V.I. Pokhmurs’kyi, I.M. Zin, S.B. Layon, L.M. Bilyi: Synergistic Effect of Phosphate and Calcium-Containing Pigments on the Corrosion Resistance of Galvanized Steel, Materials Science, **39**, pp. 153–160 (2003)
24. S.A. Greenberg: Reaction between Silica and Calcium Hydroxide Solutions. I. Kinetics in the Temperature Range 30 to 85°1, The Journal of Physical Chemistry, **65**, pp. 12–16 (1961)
25. D.V. Quang, P.B. Sarawade, A. Hilonga, J.K. Kim, Y.G. Chai, S.H. Kim, J.Y. Ryu, H.T. Kim: Preparation of silver nanoparticle containing silica micro beads and investigation of their antibacterial activity, Applied Surface Science, **257**, pp. 6963–6970 (2011)
26. S.A. Greenberg, T.N. Chang: Investigation of the Colloidal Hydrated Calcium Silicates. II. Solubility Relationships in the Calcium Oxide-Silica-Water System at 25°, The Journal of Physical Chemistry, **69**, pp. 182–188 (1965)
27. I.M. Zin, S.B. Lyon, V.I. Pokhmurskii: Corrosion control of galvanized steel using a phosphate/calcium ion inhibitor mixture, Corrosion Science, **45**, pp. 777–788 (2003)
28. B. Chico, J. Simancas, J.M. Vega, N. Granizo, I. Díaz, D. de la Fuente, M. Morcillo: Anticorrosive behaviour of alkyd paints formulated with ion-exchange pigments, Progress in Organic Coatings, **61**, pp. 283–290 (2008)
29. X. Li, J. Chang: A novel hydrothermal route to the synthesis of xonotlite nanofibers and investigation on their bioactivity, Journal of Materials Science, **41**, pp. 4944–4947 (2006)
30. L.Z. Pei, L.J. Yang, Y. Yang, C.G. Fan, W.Y. Yin, J. Chen, Q.F. Zhang: A green and facile route to synthesize calcium silicate nanowires, Materials Characterization, **61**, pp. 1281–1285 (2010)
31. V. Kasselouri, N. Kouloumbi, T. Thomopoulos: Performance of silica fume-calcium hydroxide mixture as a repair material, Cement and Concrete Composites, **23**, pp. 103–110 (2001)
32. S. Lowell, J.E. Shields, M.A. Thomas, M. Thommes: Characterization of porous solids and powders: Surface area, pore size and density, in, Kluwer Academic Publishers, Dordrecht, 2004.
33. G. Cao: Nanostructures & Nanomaterials, in, Imperial College Press, London, 2004.
34. J.J. Chen, J.J. Thomas, H.F.W. Taylor, H.M. Jennings: Solubility and structure of calcium silicate hydrate, Cement and Concrete Research, **34**, pp. 1499–1519 (2004)
35. I. Gunnarsson, S. Arnórsson: Amorphous silica solubility and the thermodynamic properties of H4SiO°4 in the range of 0° to 350°C at Psat, Geochimica et Cosmochimica Acta, **64**, pp. 2295–2307 (2000)